Available online at www.sciencedirect.com
ScienceDirect
Polymer 48 (2007) 4114–4122
polymer
www.elsevier.com/locate/polymer

Effect of the cross-linking degree on the morphology of poly(NIPAAm-*co*-AAc) hydrogels

Regiane da Silva, Marcelo Ganzarolli de Oliveira*

Chemistry Institute, State University of Campinas, UNICAMP, CP 6154, CEP 13083-970, Campinas, SP, Brazil

Received 21 November 2006; received in revised form 27 April 2007; accepted 5 May 2007
Available online 13 May 2007

Abstract

Hydrogels of poly(*N*-isopropylacrylamide) co-polymerized with acrylic acid [P(NIPAAm-*co*-AAc)] were synthesized with cross-linking degrees of 2–7% using (*N*,*N*′-methylenebisacrylamide). SEM micrographs revealed that the morphology of dry hydrogels changes from interconnected spherical pores to channel-like pores, with the change in the cross-linking degrees from 3 to 5%. The change in morphology is associated with a significant change in the swelling ratio. It was found that the diffusion rates and permeabilities of methylene blue (MB) through the hydrogel with channel-like pores are significantly higher if the main axes of the pores are oriented parallel to the flow of MB molecules, than if it is oriented perpendicularly. These results show that different morphologies can be obtained by controlling the cross-linking degree of P(NIPAAm-*co*-AAc) hydrogels in a narrow range around 5% and by performing the polymerization reaction in moulds placed in horizontal and vertical positions, opening a new perspective for modulating their properties in applications as matrices for controlled release of drugs or as membranes for separation processes.

Keywords: Poly(*N*-isopropylacrylamide); Hydrogels; Morphology

1. Introduction

Non-biodegradable hydrogels can have several applications as biomaterials, including scaffolds used as cellular culture supports, both in vitro and in vivo [1–3], coatings of cell plates used to promote controlled cell detachment [4,5] and matrices for the controlled release of drugs in target tissues [6]. In such applications, hydrogels must fulfill a number of requirements. They must be biocompatible and well tolerated by human tissue; their hydrophilic/hydrophobic balance must allow the adherence and growth of cells and they must provide an adequate chemical environment in order to keep the differentiated cell function, in the case of their use as scaffolds [7]. These abilities are largely determined by surface properties like surface charge and free energy and by the amount of water they are capable to absorb [8] that in turn, determines the absorption and diffusion of solutes through the hydrogel and the adsorption of proteins in cultured medium [9]. The amount of water absorbed by hydrogels is limited by their ability of undergoing elastic network expansion, which can be controlled by controlling the cross-linking degree during the synthesis of chemically cross-linked hydrogels [10]. More recently, a special interest has been devoted to stimuli-responsive hydrogels, known as intelligent hydrogels. Among the various responses that can be obtained, those hydrogels which respond to temperature and pH have potential to be used as drug delivery systems, once they can be loaded with the drug solution through absorption and the rate of drug release can be controlled by changing the temperature or the pH of the medium where they are located [6,11–14]. Poly(*N*-isopropylacrylamide) [P(NIPAAm)] form well known thermosensitive hydrogels. When heated above 32 °C, P(NIPAAm) hydrogels exhibit a hydrophilic/hydrophobic transition in aqueous medium (Lower critical solution temperature – LCST) [8,15]

* Corresponding author. Tel.: +55 19 35213132; fax: +55 19 35213023.
E-mail address: mgo@iqm.unicamp.br (M. Ganzarolli de Oliveira).

0032-3861/$ - see front matter © 2007 Elsevier Ltd. All rights reserved.
doi:10.1016/j.polymer.2007.05.010

characterized by the collapse of the three-dimensional gel structure with consequent expulsion of the solvent. This property can thus be useful for promoting the fast release of drugs in solution and has led to strategies for modulating the LCST for biomedical applications [16–18]. One of these strategies is copolymerizing NIPAAm with acrylic acid (AAc) [6,19]. In addition, their LCST, swollen behavior and the rate of drug release are affected by the amount of co-polymerized AAc [20]. These properties are ultimately correlated to the morphology of the polymeric network of the hydrogels. Although hydrated P(NIPAAm-*co*-AAc) hydrogels are macroscopically isotropic to the naked eye, the dried hydrogels reveal an intricate microscopic porous structure composed of interconnected cells that can have different geometries. The morphology of these so-called ''superporous hydrogels'' can be a key factor in defining whether the absorption or release of solutes will be mainly driven by simple diffusion or by capillary forces [21]. In addition, morphology and surface topography of the gel structure can also affect culture cells by guiding cell spreading. In this respect, membranes or scaffolds with oriented channel-like pores are desirable to provide nutrient supply during cell culture.

Establishing a correlation between the morphology of P(NIPAAm-*co*-AAc) hydrogels and their swelling and diffusion behaviors, as well as understanding how the morphology is affected by their cross-linking degree, is fundamental for planning the use of such materials as mentioned above.

In this work, membranes of P(NIPAAm-*co*-AAc) hydrogels were synthesized in aqueous solutions using different amounts of *N*,*N*′-methylenebisacrylamide (BIS) as a cross-linking agent. Hydrogels were characterized regarding their swelling behavior and LCST in hydrating conditions. The morphology of dry hydrogels changed from interconnected spherical pores to channel-like pores, with the change in the cross-linking degrees from 3 to 5%. The channel-like pore morphology led to significantly higher diffusion rates and permeabilities of methylene blue (MB) in membranes with the main axis of the pores oriented parallel to the flux of MB molecules, compared to the perpendicular orientation.

2. Experimental

2.1. Materials

N-Isopropylacrylamide (NIPAAm) monomer, stabilized 99% and acrylic acid (AAc) monomer, stabilized 99.5% (Acros organics) were previously purified twice by recrystallization in hexane and by vacuum distillation at 39 °C and 10 mmHg, respectively. *N*,*N*′-Methylenebisacrylamide (BIS) monomer, stabilized 99% (Acros organics) was used as a cross-linking agent, and *N*,*N*,*N*′,*N*′-tetramethylethylenediamine (TEMED), 99% (Plusone-Pharmacia Biotech), was used as an accelerator, sodium persulfate ($Na_2S_2O_8$), P.A. (Synth), was used as initiator of polymerization, and phosphate buffer saline (PBS) with pH 7.4 (Sigma) was used as-received. Methylene blue (MB) was purchased from Synth, Brasil. Gaseous nitrogen (N_2) was purchased from Air Liquid and Parafilm was purchased from Pechiney-Plastic Packaging, Menasha, WI. The experiments were carried out using analytical grade water from Millipore Milli-Q gradient filtration system.

2.2. Synthesis of P(NIPAAm) and P(NIPAAm-co-AAc)

P(NIPAAm) was synthesized in aqueous solutions containing 5% wt/wt of NIPAAm in the presence of sodium persulfate (43 μmol L^{-1}) and TEMED (2.5 mol L^{-1}). NIPAAm and persulfate were kept under constant stirring and nitrogen bubbling for 1 h at room temperature. After this period, TEMED, was added and the solution was kept under the same condition for 24 h. P(NIPAAm) obtained was purified by precipitation, by throwing the solution onto hot water (60 °C) [22]. The precipitated polymer was removed from the water with tweezers and this procedure was repeated twice. The purified P(NIPAAm) was dried in a desiccator using silica-gel at room temperature for 48 h. P(NIPAAm-*co*-AAc) hydrogels were synthesized in aqueous solutions containing 80 mol% NIPAAm/mol total monomer, 20 mol% AAc/mol total monomer, and 2, 3, 5 and 7 mol% BIS/mol (total monomer + cross-linker), in the presence of sodium persulfate (43 μmol L^{-1}) and TEMED (2.5 mmol L^{-1}) (Table 1). All the formulations were moulded as thin membranes. In each case, the appropriate amounts of NIPAAm, AAc, $Na_2S_2O_8$ and BIS were initially dissolved in water and the solutions were kept under constant stirring and nitrogen bubbling for 1 h at room temperature. After this period, TEMED was added. The final solutions were inserted in moulds composed of two glass plates (10 × 5 cm) kept apart by a rubber spacer 3 mm thick. The moulds were positioned in two different situations: (1) with the plane of the glass plates in the vertical position and (2) with the plane of the glass plates in the horizontal position. After filling with reactants the moulds were kept closed for 24 h at room temperature for the cross-linking reactions (Fig. 1(a)). The hydrogel membranes obtained were immersed in deionized water until reaching the swelling equilibrium. The membranes were further purified by several washings with deionized water [23,24], immersed in liquid nitrogen and freeze-dried for 48 h [25].

2.3. Infrared spectroscopy

Infrared spectra of P(NIPAAm-*co*-AAc) hydrogels and of NIPAAm and AAc monomers were recorded with an FT-IR (Bomem B-100 Hartmann & Braun, CA-USA) spectrophotometer at room temperature. The spectrum of AAc was

Table 1
Concentrations of reagents used in the synthesis of hydrogels with cross-linking degrees of 2, 3, 5 and 7%

Cross-linking degree (%)	NIPAAm (mmol L^{-1})	AAc (mmol L^{-1})	BIS (mmol L^{-1})
2	400	100	10
3	400	100	15
5	400	100	25
7	400	100	35

[TEMED] = 43 μmol L^{-1} and [$Na_2S_2O_8$] = 2.5 mmol L^{-1}.

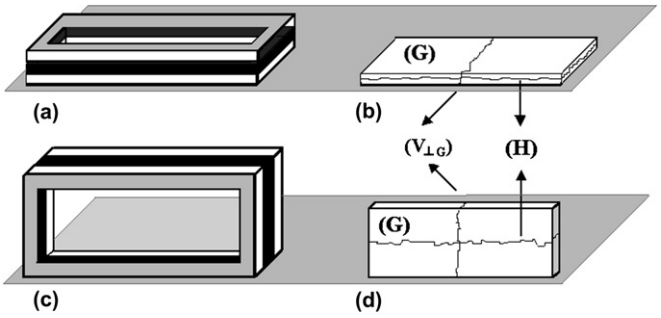

Fig. 1. Scheme of the mould of cross-linked P(NIPAAm-*co*-AAc) hydrogel membranes with the mould positioned horizontally (a and b) and vertically (c and d), relative to the bench surface. ($V_{\perp G}$) is the vertical fracture surface perpendicular to the plane of the glass plate; (G) is the surface in contact with the glass plate; (H) is the horizontal fracture surface.

obtained using a capillary film of AAc between two calcium fluoride (CaF_2) windows. The spectra of P(NIPAAm) monomer and of freeze-dried P(NIPAAm-*co*-AAc) hydrogel were obtained in pressed KBr disks (1% wt/wt) [26]. All samples were analyzed in the range 4000–1000 cm^{-1}.

2.4. Morphological analysis

For the morphological characterization, hydrogels with cross-linking degrees of 3 and 5% were kept in deionized water at 25 °C for 48 h to reach swelling equilibrium and at 37 °C for 4 h. The swollen hydrogels were cut in slices (2 cm × 3 mm × 1 mm) and frozen in liquid nitrogen in order to obtain the mechanical fracture surfaces according to Fig. 1(b) and (c). The fractured samples were freeze-dried for 24 h in order to preserve the open microporous structure of the hydrogels [25,27] and metalized with gold. Slices of the dried samples (2 cm × 3 mm × 1 mm) were also cut according to the surfaces of Fig. 1(b) and (c) using a scalpel, in order to obtain thin sheets with flat surfaces. Photomicrographies of cryoscopically fractured samples and of sliced samples of the dried hydrogels were examined using a Scanning Electron Microscopy (SEM-JSM 6360-LV, Tokyo, Japan) [17,19] with magnifications ranging from 18 to 1000×.

2.5. Swelling equilibrium behavior

The swelling ratio (Q) was calculated as the ratio of weight of swollen hydrogel (W_s), by the weight of dried hydrogel (W_d) [19,24] in PBS solution (pH 7.4), deionized water (pH 6.4) and HCl solution (pH 3.5). Hydrogel samples were immersed in these solutions at 25 °C for 2 days, until the swelling equilibrium was reached and subsequently weighted. Error bars represent the standard error of the mean of duplicates and triplicates.

2.6. Lower critical solution temperature (LCST) measurements

LCSTs were measured spectrophotometrically, based on the cloud point method [8]. Aqueous P(NIPAAm) solution (5% wt/wt) or hydrogels (swollen in deionized water HCl solution or PBS solution, for 48 h) were transferred to a quartz cuvette (1 cm path length) and heated from 25 to 40 °C at a heating rate of 0.25 °C min^{-1}, using a Peltier-controlled diode array spectrophotometer (Hewlett-Packard, Model 8453, Palo Alto, CA, USA). Absorbance changes at $\lambda = 700$ nm, referenced against air, were recorded and LCSTs were measured as the first discontinuity in the absorbance vs. temperature, caused by light scattering due to phase separation.

2.7. Diffusion measurements

The diffusion of MB across membranes of hydrogel with cross-linking degree of 5%, was measured in a side-by-side diffusion apparatus consisting of two cylindrical glass-stirred diffusion cells (60 mL each) [24,28–30]. The swollen membranes were placed between the two cells and their ends were covered with Parafilm. The assembly was kept in a thermostatized room at 25 ± 1 °C during the experiments. The membranes were positioned in two different orientations: (a) with the main axis of the tubular pores parallel (∥) and (b) with the main axis of the tubular pores perpendicular (⊥), relative to the flow of MB molecules from one cell to the other. The temperature of 25 °C was selected in order to allow a comparison between the MB flow across membranes with pores opened, i.e. below LCST, in these two orientations. Membranes were 2.5 mm thick and the open area between the half-cells was $A = 3.46$ cm^2. Before starting the measurements, the membranes were immersed in MB solution 2.7×10^{-4} mol L^{-1} at room temperature to reach absorption equilibrium and subsequently washed with deionized water to remove free MB molecules. The donor cell was filled with a 2.7×10^{-5} mol L^{-1} MB solution and the receptor cell was filled with deionized water. The increase in MB concentration in the receptor cell was monitored spectrophotometrically at 665 nm with a diode array UV–vis spectrophotometer (Hewlett-Packard, model 8453, Palo Alto, CA, USA) every 30 min for 4 h. The samples' absorbance was determined immediately upon removal of the aliquots from the receptor cell. After the absorbance measurements the aliquots were returned to the receptor cell.

3. Results and discussion

3.1. Infrared spectroscopy

Fig. 2 shows a comparison among the infrared spectra of the hydrogel with cross-linking degree of 2%, NIPAAm and AAc. The absorption band of the hydrogel at ca. 1710 cm^{-1}, can be assigned to the C=O vibration of AAc. The broad band with maximum at ca. 1650 cm^{-1} can be assigned to the overlapping of the NIPAAm and AAc absorptions in the range 1610–1670 cm^{-1} and the band at 1550 cm^{-1} can be assigned to the N–H vibration of NIPAAm. Thus, the presence of these bands in the spectrum of the purified P(NIPAAm-*co*-AAc) hydrogel confirms the copolymerization reaction between NIPAAm and AAc monomers.

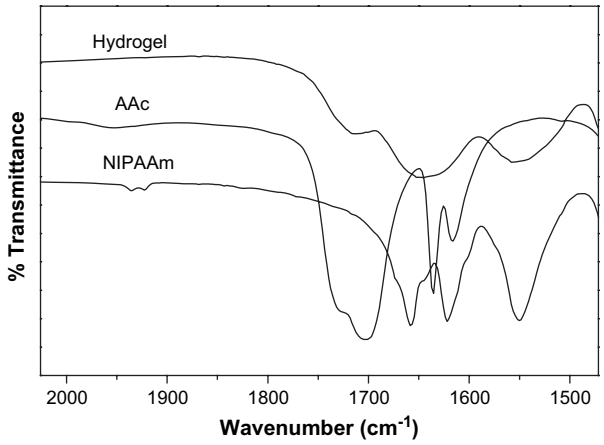

Fig. 2. FT-IR spectra of P(NIPAAm-*co*-AAc) hydrogel with cross-linking degree of 2%, NIPAAm and AAc monomers. The vertical axis was shifted to avoid the overlapping of the curves. The percentage of transmission scales varied in the range 80–50%.

3.2. Morphological analysis

Figs. 3–5 show the SEM micrographs of cryogenic fracture surfaces of hydrogels with cross-linking degrees of 3 and 5% lyophilized from equilibrium swelling conditions at 25 and 37 °C and pH 6.4. The morphological analysis was focused on these two hydrogels because they show the greater change in swelling behavior at pH 6.4 (see below) allowing a better investigation of the correlation between morphology and swelling behavior. Fig. 3 shows the SEM micrographs of hydrogels with cross-linking degrees of 3 and 5% below and above LCST. Below LCST (i.e. 25 °C) the horizontal fracture surfaces (Fig. 3(a) and (c)) display highly porous structures with similar pore diameters: 33 ± 5 μm for the hydrogel with cross-linking degree of 3% and 38 ± 6 μm for hydrogel with cross-linking degree of 5% [15]. Above the LCST (i.e. 37 °C), the collapse of the P(NIPAAm) units induces a great hydrophobic environment responsible by the fast contraction of the hydrogel [31], which assumes a shrunken state [23]. This contraction can be clearly seen in the micrographs of Fig. 3(b) and (d), which were obtained after the achievement of swelling equilibrium above LCST. The collapsed hydrogels still display porous structures but with much smaller pore diameters [15]. There is, however, a very significant difference between the pore morphology of hydrogels with cross-linking degrees of 3 and 5% below LCST. In the hydrogel with cross-linking degree of 3% (Fig. 3(a)) the pore structure has a sponge-like shape with spherical open and interconnected cells. On the other hand, in the hydrogel with cross-linking degree of 5% (Fig. 3(c)) the pore structure is composed of channel-like pores whose main axes are lined with the vertical axis of the mould, forming a regular and oriented tubular microstructure. The generation of these two different morphologies was confirmed in several different preparations and in hydrogels with cross-linking degrees of 2 (spherical cells) and 7% (tubular cells) (see Supplementary material). These features can be better observed in Figs. 4 and 5, which show the vertical fracture surfaces (Figs. 4(a) and 5(a)) and details of the horizontal fracture surfaces at magnifications of 1000× (Figs. 4(b) and 5(b)) for the swollen hydrogels below LCST. It must be noted that the interconnectivity of the pores

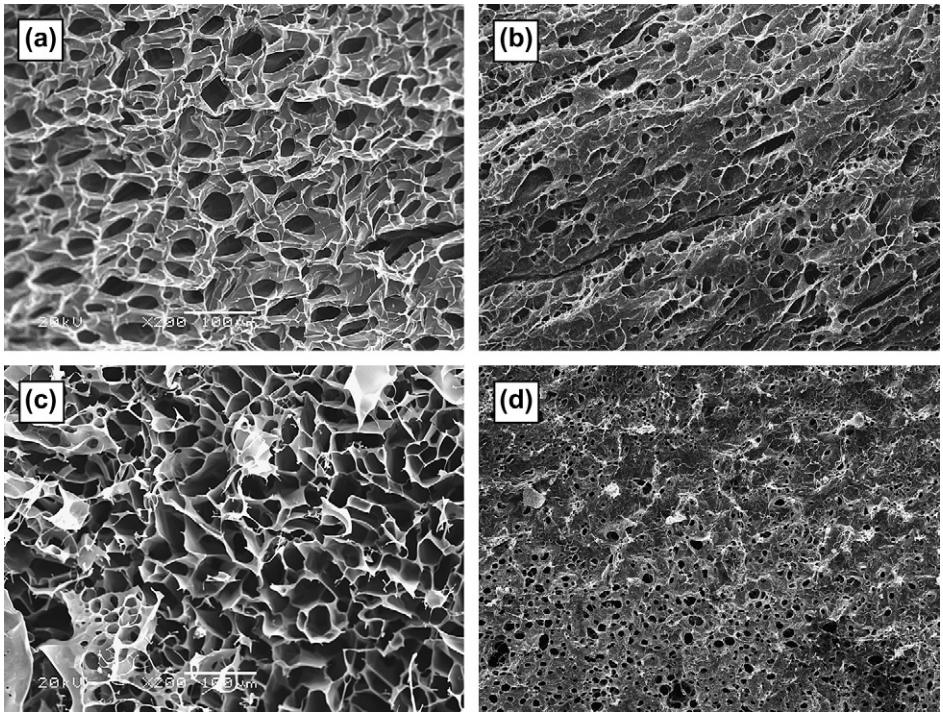

Fig. 3. SEM micrographs of hydrogels with cross-linking degrees of 3 and 5% after reaching the swelling equilibrium below LCST at 25 °C (a and c, respectively) and above LCST at 37 °C (b and d, respectively). Horizontal fracture surface (*H*), magnification: 200×.

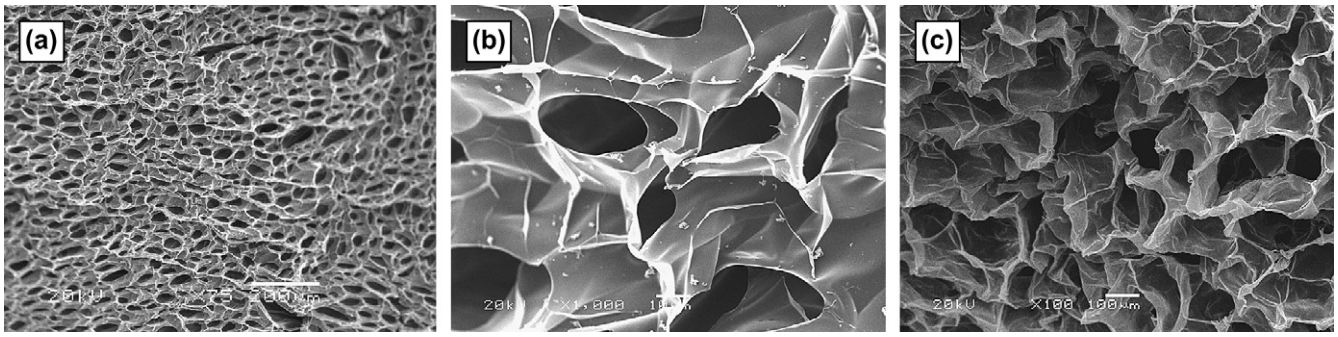

Fig. 4. SEM micrographs of hydrogel with cross-linking degree of 3% after reaching the swelling equilibrium below LCST at 25 °C. (a) Vertical fracture surface perpendicular to the plane of the glass plate ($V_{\perp G}$), magnification: 75×; (b) horizontal fracture surface (H), magnification: 1000×; (c) surface in contact with the glass plaque (G), magnification: 100×.

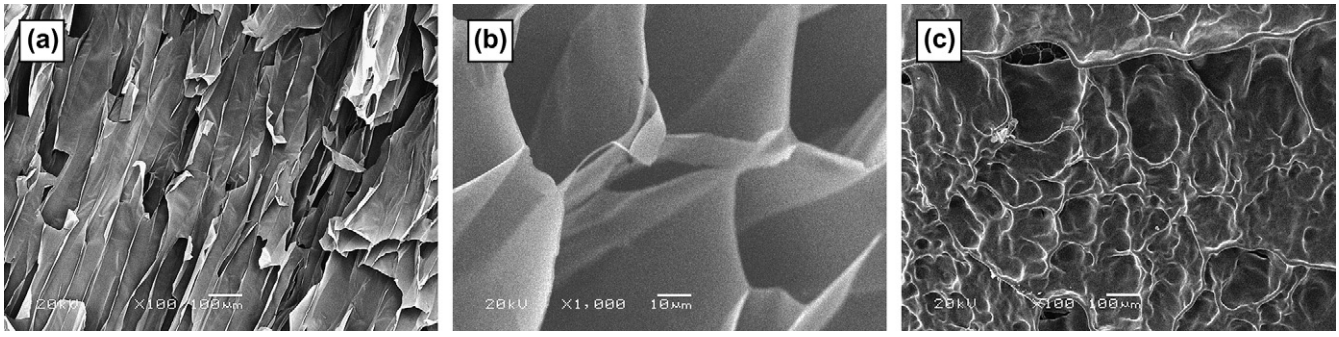

Fig. 5. SEM micrographs of hydrogel with cross-linking degree of 5% after reaching the swelling equilibrium below LCST at 25 °C. (a) Vertical fracture surface perpendicular to the plane of the glass plate ($V_{\perp G}$), magnification: 100×; (b) detail of the tubular pore structure in the horizontal fracture surface (H), magnification: 1000×; (c) surface in contact with the glass plaque (G), magnification: 100×.

in the sponge-like structure is expected to be higher than that in the channel-like structure. Such characteristic must allow the diffusion of solutes in every direction with similar rates. On the other hand, the channel-like structure must allow higher diffusion rates along the pore axis. It must be emphasized that the cryogenic method used to exam the surface of the fractured hydrogels preserves their microstructure, as already pointed out by others [25]. Thus, the observed difference between the two morphologies is real and not an artifact caused by drying. The possibility of synthesizing hydrogels with sponge-like or channel-like structures could be used for modulating the rate of release of solutes in local or topical applications. Figs. 4(c) and 5(c) show another morphological feature of hydrogels with cross-linking degrees of 3 and 5%. It can be seen that the faces of the membranes formed in contact with the glass plates are mainly coated by a continuous film with relatively few apertures. This seems to be a result that does not depend on the cross-linking degree and is probably induced by the glass surface. Effects of the chemical nature of the mould surface on the morphology of superporous P(NIPAAm-*co*-AAc) hydrogels were already reported and assigned to the establishment or not of specific interactions between the surface and the polymer [21].

Still, examination of the vertical fracture surface perpendicular to the plane of the glass plate in membranes prepared with the mould in the vertical and in the horizontal positions reveals a new feature of the tubular structure of the hydrogel with cross-linking degree of 5%. First, in both mould positions, the main axes of the pores are aligned vertically relative to the plane of the bench surface. That is, there is a clear gravitational effect in the morphogenesis of the tubular pores. Second, in membranes prepared with the mould in the horizontal position, the pore growth during the polymerization reaction, apparently starts at both glass surfaces and proceeds toward the center of the membrane, where the two front lines of polymerization meet, defining a sharp surface, exactly at the medial plane of the membrane thickness. These meeting polymerization fronts lead to the formation of an apparently continuous wall parallel to the glass surface at this plane, as one can see in the SEM picture of Fig. 6(a) and (b). (See also another example in Fig. 4(a) and (b) in Supplementary material.) This feature suggests that the glass surface acts as a kind of ‘‘nucleating’’ surface for the initiation of the polymerization and phase separation processes. Another evidence that this effect is operative is the formation of a continuous membrane adjacent to both glass surfaces as one can see in the micrograph of hydrogel with cross-linking degree of 5% in Fig. 5(c).

In membranes prepared with the mould in the vertical position, the pores apparently cross the entire height of the mould (see Fig. 2 in Supplementary material). In this case, it is not possible to find any evidence that the pores also grow during polymerization reaction from both glass surfaces toward the center of the membrane, for if this happens, the vertical meeting fronts will be masked by the vertical pore walls. Thus, the

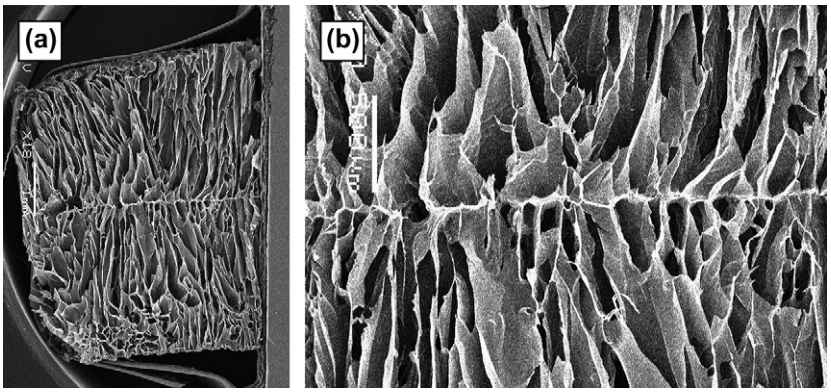

Fig. 6. SEM micrograph of a hydrogel membrane with cross-linking degree 5% after reaching the swelling equilibrium below LCST at 25 °C, prepared with the mould in the horizontal position. (a) Vertical fracture surface perpendicular to the plane of the glass plate ($V_{\perp_G}$), showing the formation of a horizontal divisor membrane at the medial plane of the membrane. Magnification: 18×; (b) the same as (a). Magnification: 30×.

length of the pores is about half of the thickness of the membranes, for membranes prepared with the moulds in the horizontal position and is approximately the height of the mould for membranes prepared with the moulds in the vertical position. It must be noted, however, that these conclusions remain valid only for the membranes of 3 mm thickness used in this work and cannot be extrapolated to other thicknesses without previous investigation.

3.3. Lower critical solution temperature (LCST)

Incorporation of ionizable acrylic acid (AAc) groups in the structure of P(NIPAAm) hydrogels is known to increase their sensitivity to temperature, pH and ionic strength [32]. In the present case, the P(NIPAAm-*co*-AAc) copolymers obtained displayed an increased solubility, reflected in the shift of the LCST, from 32 °C for P(NIPAAm) solution to 37 °C for P(NIPAAm-*co*-AAc) hydrogels with cross-linking degrees of 3 and 5%, at pH 6.4 (Fig. 7). It can also be observed in Fig. 7 that the LCST was not significantly affected by using 3 or 5 mol% BIS/mol as a cross-linking agent. The LCST is a parameter associated with the reversible volume phase transition (VPT) of P(NIPAAm), which is caused by the cleavage of hydrogen bonds between hydrophilic groups of the polymer and surrounding water molecules, with increasing temperature [33], a phenomenon driven by the increase in entropy due to the release of the hydrating water molecules [34].

3.4. Swelling equilibrium behavior

Fig. 8 shows the swelling ratios of P(NIPAAm-*co*-AAc) hydrogels prepared with 2, 3, 5 and 7 mol% BIS/mol in PBS solution (pH 7.4), deionized water (pH 6.4) and HCl solution (pH 3.5). The low swelling ratios observed at pH 3.5 can be assigned to the reduced expansion capability of the hydrated P(NIPAAm-*co*-AAc) chains, due to the protonation of the carboxyl groups of the AAc units, whose pK_a is 4.25 [34]. In solutions at pHs above 4.25, the swelling ratios increase expressively. This effect is more evident when comparing the swelling ratios at pHs 3.5 and 6.4. At pH 6.4 the carboxylic groups of AAc units are deprotonated and negatively charged. The coulombic repulsions among these groups increase the Donnan potential inside the network as a whole contributing to the achievement of a greater expansion of the network and thus to higher swelling ratios [25]. Interestingly, in PBS solution with pH higher than 6.4, intermediate swelling ratios were obtained. This result can be interpreted by considering that in this saline medium the carboxylate groups ($-COO^-$) are partially neutralized by the shielding effect of the sodium ions, reducing the Donnan potential in the network and thus its expansion. In this condition, the elastic strength counteracts the network expansion [10], and leads to higher compression modules [19]. This result highlights the possibility of modulating the swelling/deswelling properties of P(NIPAAm-*co*-AAc) hydrogels by using media with different pHs or salinity, which may be important in applications aimed at releasing drugs locally on tissues, from swelled hydrogels.

Fig. 8 also shows the effect of the extent of cross-linking with BIS on the swelling ratio. It was observed that in all three

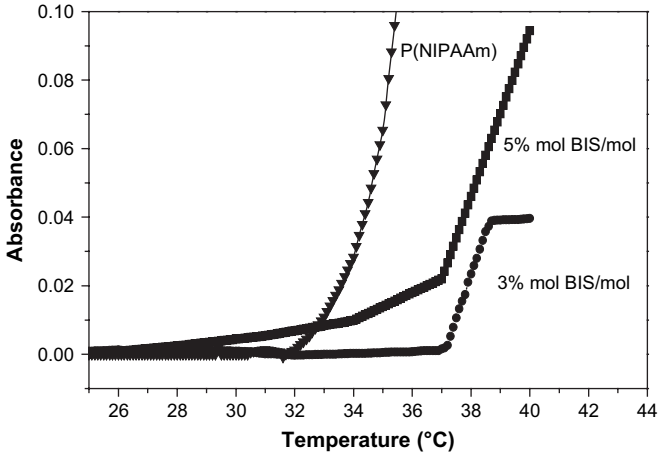

Fig. 7. Lower critical solution temperature (LCST) of swollen P(NIPAAm-*co*-AAc) hydrogels with cross-linking degrees of 3 and 5% and of P(NIPAAm) solution (5% wt/wt) without AAc, measured spectrophotometrically through the absorption changes at 700 nm with increasing temperature. Heating rate = 0.25 °C min^{-1}.

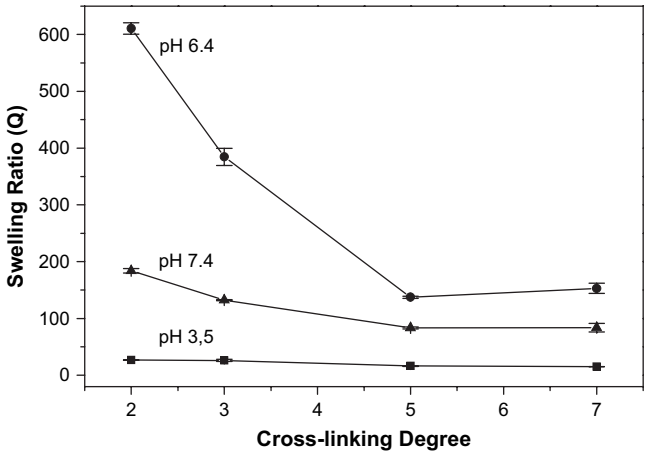

Fig. 8. Swelling ratio of hydrogels with cross-linking degrees of 2, 3, 5 and 7% in solutions with different pHs after reaching the swelling equilibrium below LCST at 25 °C. Error bars are the SEM of triplicates.

pHs studied, the swelling ratio decreases with increasing cross-linking degrees from 2 to 5 mol% BIS/mol. This result is less evident at pH 3.5, where the swelling ratios are low, but this trend can also be identified in this condition. What calls attention in these results is that increasing the cross-linking degrees from 5 to 7 mol% BIS/mol did not further decrease the swelling ratio, suggesting that a transition in the swelling behavior is achieved at a cross-linking degree of 5%. An apparent correlation can be established between the morphology of hydrogels with cross-linking degrees of 3 and 5% and this transition in the swelling behavior. The higher swelling ratio of hydrogels with cross-linking degrees below 5% is possibly associated with the higher three-dimensional radial expansion capability of spherical cells, compared to the tubular-like cells of hydrogels with cross-linking above 5%. In the latter, the expansion is restricted in the vertical axis relative to the transversal plane of the pores, which can undergo bi-dimensional radial expansion.

3.5. Diffusion measurements

The diffusion of MB across the membranes of the 5% cross-linked hydrogel was used to characterize the tubular morphology obtained in this case and to compare the diffusion behavior in this morphology with that obtained in hydrogel with 3% cross-linked hydrogel with non-channel, interconnected pore structure. As MB is a cationic dye [22], it adsorbs strongly on the negatively charged P(NIPAAm-*co*-AAc) chains. For this reason, the membranes were previously soaked in MB solution for one day, in order to achieve absorption equilibrium. After this time, P(NIPAAm-*co*-AAc) membranes displayed the dark blue coloration of the original MB solution and the dye solution became only slightly blue. The nature of the interactions between the cationic MB molecules and acrylamide hydrogels has already been discussed in other works [22,35]. They involve not only the electrostatic interactions between the cationic group of MB and the carboxyl group of the hydrogel, but also hydrophobic interactions between the conjugated aromatic system of MB and the methyl groups of the hydrogel. After absorption equilibrium has been achieved, the diffusion of free MB molecules is limited by their passage through the water-filled regions, or free volumes, inside the pore walls. Such diffusion behavior is well known to change strongly below and above the LCST. In the present case the measurements were done below LCST.

The diffusion rates and corresponding permeabilities of the 5% cross-linked hydrogel were measured in membranes mounted in the diffusion cell with the main axis of the pores oriented parallel and perpendicularly relative to the MB flow (Figs. 9 and 10). In these two different situations, it can be expected that MB displays different kinetics of diffusion, for in the perpendicular orientation, the number of pore walls that must be crossed by MB molecules is larger than in the parallel orientation, for the same membrane thickness. As discussed above, the tubular pores are not continuous and do not cross the entire membrane thickness (Fig. 5(a)). Thus, even in the parallel orientation, the diffusing MB molecules have to cross pore membranes. The influence of pore orientation of 5% cross-linked hydrogel in the diffusion rate of MB in aqueous solution is shown in Figs. 9(a) and 10(a). It can be seen that the diffusion rate of MB is ca. 10 times higher in the membrane with tubular pores oriented parallel than in the membranes with the pores oriented perpendicularly, relative to the flow of MB molecules. This difference is also reflected in the bar graph of Fig. 10(b) which shows the corresponding permeabilities, calculated through Eq. (1):

$$P = \left(\frac{\partial c}{\partial t}\right)\frac{Vd}{C_o A} \tag{1}$$

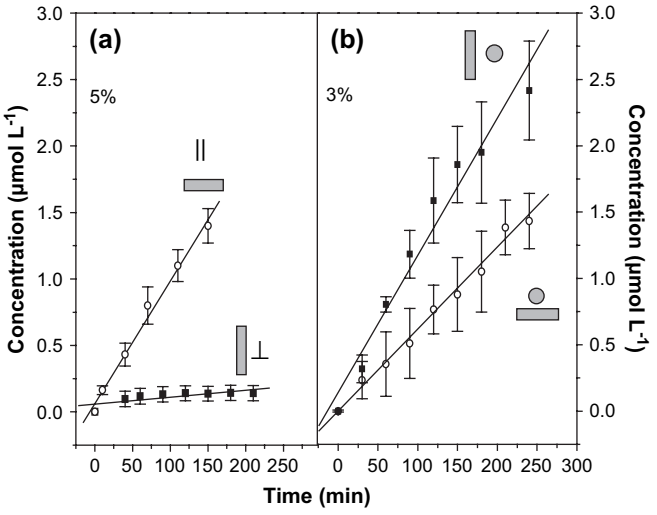

Fig. 9. Diffusion of methylene blue (MB) at 25 °C as a function of time across membranes of hydrogels with cross-linking degrees of 5% (a) and 3% (b) for membranes prepared with the mould positioned in the horizontal (▭) and vertical (▯) positions. In (a), ∥ and ⊥ indicate that the flow of MB is parallel and perpendicular relative to the main axis of the tubular pores, respectively. In (b), (◎) indicates that the membranes have interconnected spherical pores. The straight lines were obtained by linear regression of the experimental points. MB concentration in the donor cell was 2.7×10^{-5} mol L^{-1} in all cases.

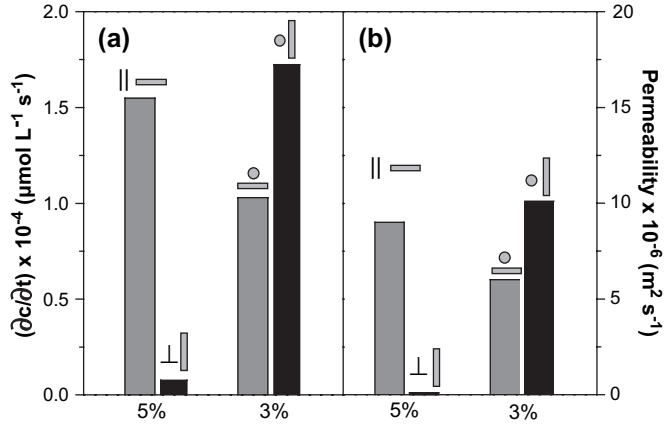

Fig. 10. Diffusion rate ($\partial c/\partial t$) (a) and permeability (b) of methylene blue (MB) at 25 °C across membranes of hydrogels with cross-linking degrees of 5% (a) and 3% (b) for membranes prepared with the mould positioned in the horizontal (▬) and vertical (▮) positions. In (a), ∥ and ⊥ indicate that the flow of MB is parallel or perpendicular relative to the main axis of the tubular pores, respectively. In (b), (●) indicates that the membranes have interconnected spherical pores. MB concentration in the donor cell was 2.7×10^{-5} mol L^{-1} in all cases.

where, ($\partial c/\partial t$) is the slope of the straight lines obtained in the linear regressions of Fig. 9, V and C_o are the volume of the donor cell compartment and the concentration of MB donor solution, respectively, and A and d are the area and the thickness of the membrane, respectively [24,28]. It can be considered that, in the experimental conditions used, the MB concentration in the donor cell remains practically constant (it decreases by less than 6%) and the concentration in the receptor cell is always very low, leading to a practically constant concentration gradient between both sides of the membrane. In addition, in the concentration of the MB solution used (2.7×10^{-5} mol L^{-1}), MB is in its monomeric form. This was confirmed by obtaining the UV–vis spectrum of the solution, which displayed only the absorption band due to the monomer at 665 nm [36] (data not shown). The permeability of MB in the 5% cross-linked hydrogel is ca. 45 times higher in the membrane with tubular pores oriented parallel than in the membranes with the pores oriented perpendicularly, relative to the flow of MB molecules. The significant change observed in the diffusion rates, and permeabilities to MB, depending on the membrane orientation in the diffusion cell, confirms the existence of long oriented tubular pores in the hydrogels synthesized with cross-linking degrees of 5% (or higher), according to what can be seen in the morphologies as shown in Figs. 4–6.

Figs. 9 and 10 also show the diffusion behavior of MB solution in the 3% cross-linked hydrogel with interconnected spherical pores. Although SEM micrographs of hydrogel 3% show an apparent isotropic distribution of non-channel interconnected pores that doesn't depend on the position of the mould during the preparation of the membranes, diffusion parameters changed depending on the position of the mould. In this case, diffusion rates ca. 1.8 times higher and corresponding permeabilities ca. 1.7 higher (Figs. 9(b) and 10(b), respectively) were obtained for membranes of hydrogel 3 prepared with the mould in the vertical position. Although these differences are much smaller than those obtained for the tubular hydrogel, these results show that these membranes must also have some degree of pore orientation and that this orientation favors diffusion if the membranes are prepared with the mould in the vertical position, compared to the horizontal position.

In addition, regardless the position of the mould, the diffusion rates in the 3% cross-linked hydrogel were found to be much higher than the diffusion rates in hydrogel 5%, with the main axis of the pores oriented perpendicularly to solute flow. On the other hand, the magnitude of the diffusion rates obtained for the 3% cross-linked hydrogel approaches that of the 5% cross-linked hydrogel with the main axis of the pores oriented parallel to the solute flow. This result is also reflected in the permeability values of Fig. 10(b) and indicates that the diffusion rate depends on the number of pore walls that have to be crossed by MB molecules in their course across the membranes. The similar order of magnitude obtained for the diffusion rates in the 3% cross-linked hydrogel and in the 5% cross-linked hydrogel with pores oriented perpendicularly to solute flow, indicates that, in both cases, the solute must cross a similar number of pore walls in order to diffuse through the same membrane thickness. This is in accordance to the fact that the tubular pores do not cross the entire thickness of the membranes as discussed above.

These different morphologies, which can be obtained in P(NIPAAm-*co*-AAc) hydrogels by changing the cross-linking degree around 5%, have not been reported before in other works in the literature. There are also no reports on the effect of the position of the mould on the morphology of these hydrogels, as well as on the influence of these particular morphologies on their swelling and diffusion behaviors. However, other techniques used to modulate the morphology of P(NIPAAm) hydrogels, have already been reported. Zhang and Chu [37] for example, used a new strategy for preparing PNIPAAm gel with improved properties, by cross-linking polymerization in DMSO at low temperatures. SEM analysis of the gels obtained, revealed a microstructure much more oriented and regular than the conventional PNIPAAm gels, but still different from the tubular structure reported here. Similarly, these authors also attributed the improved swelling and deswelling kinetics and dynamic response of this hydrogel to its unique interior morphology. Zhang et al. [17] reported SEM images of freeze-dried P(NIPAAm-*co*-AAc) gels with a morphology of isotropically interconnected cells, very similar to the non-tubular morphology of the hydrogel with cross-linking degree of 3% reported here. However, these authors have only used these images to analyze the influence of the incorporation of AAc and in the pH during the copolymerization reaction in the expansion of P(NIPAAm) network and did not correlate changes in morphology with diffusion properties. Gemeinhart and colleagues [21] have described the pore structure of cross-linked P(NIPAAm) superporous hydrogels, which may display spherical interconnected pores, as well as elongated pores. However, these authors used a gas blowing technique to obtain such morphologies. These works, although using different approaches, reinforce the interest in

understanding and controlling the morphology and swelling behavior of P(NIPAAm) hydrogels. The results herein reported, underscore the influence of two new factors, which could be used to modulate the properties of P(NIPAAm-*co*-AAc), namely the cross-linking degree and the position of the mould during the polymerization process. Together with other strategies, these results may increase the potential of P(NIPAAm-*co*-AAc) hydrogels in applications for the controlled release of drugs, or as membranes for separation processes.

4. Conclusions

Sponge-like porous hydrogels of P(NIPAAm-*co*-AAc) with spherically interconnected cells can be obtained with cross-linking degrees below 5%, while hydrogels with oriented channel-like pores can be obtained with cross-linking degree of 5 or 7%. The change in morphology is associated with a significant change in the swelling behavior of the hydrogels. Diffusion rates and permeabilities of MB through the hydrogel with channel-like pores are significantly higher if the main axes of the pores are oriented parallel to the flux of MB molecules, than if it is oriented perpendicularly. These results show that different morphologies can be obtained by controlling the cross-linking degree of P(NIPAAm-*co*-AAc) hydrogels in a narrow range around 5% and by performing the polymerization reaction in moulds placed in horizontal and vertical positions, allowing the modulation of their swelling and solute diffusion behaviors.

Acknowledgments

RS holds a fellowship from Fundação de Amparo à Pesquisa do Estado de São Paulo (FAPESP), project 04/11204-4. The authors wish to thank FAPESP for financial support.

Appendix. Supplementary material

Supplementary data associated with this article can be found in the online version, at doi:10.1016/j.polymer.2007.05.010.

References

[1] Wang K, Tsai DC, Nam EK, Aitken M, Sprague SM, Patel PK, et al. J Biomed Mater Res 1998;42:491–9.
[2] Vernon B, Gutowska A, Kim SW, Bae YH. Macromol Symp 1996;109:155–67.
[3] Stile RA, Healy KE. Biomacromolecules 2001;2:185–94.
[4] Schmaljohann D, Oswald J, Jørgensen B, Nitschke M, Beyerlein D, Werner C. Biomacromolecules 2003;4:1733–9.
[5] Higuchi A, Yamamoto T, Sugiyama K, Hayashi A, Tak TM, Nakagawa T. Biomacromolecules 2005;6:691–6.
[6] Peppas NA, Bures P, Leobandung W, Ichikawa H. Eur J Pharm Biopharm 2000;50:27–46.
[7] Diego RB, Olmedilla MP, Serrano Aroca Á, Gómez Ribelles M, Monleón Prads M, Gallego Ferrer G, et al. Mater Sci Mater Med 2005;16:693–8.
[8] Schild HG. Prog Polym Sci 1992;17:163–249.
[9] Hoffman AS. Artif Organs 1995;19:458–67.
[10] Matzelle TR, Geuskens G, Kruse N. Macromolecules 2003;36:2926–31.
[11] Hoffman AS. Adv Drug Delivery Rev 2002;43:3–12.
[12] Yamashita K, Hashimoto O, Nishimura T, Nango M. React Funct Polym 2002;51:61–8.
[13] Chilkoti A, Dreher MR, Meyer DE, Raucher D. Adv Drug Delivery Rev 2002;54:613–30.
[14] Shin BC, Kim SS, Ko JK, Jegal J, Lee BM. Eur Polym J 2003;39:579–84.
[15] Park TG, Hoffman AH. Biotechnol Progr 1994;10:82–6.
[16] Gutowska A, Bae YH, Jacobs H, Feije J, Kim SW. Macromolecules 1994;27:4167–75.
[17] Zhang X-Z, Yang Y-Y, Wang F-J, Chung T-S. Langmuir 2002;18:2013–8.
[18] Vernon B, Kim SW, Bae YH. J Biomed Mater Res 2000;51:69–79.
[19] Zhang X-Z, Sun G-M, Wu D-Q, Chu C-C. J Mater Sci Mater Med 2004;15:865–75.
[20] Zhang X-Z, Wu D-Q, Chu C-C. Biomaterials 2004;25:3793–805.
[21] Gemeinhart RA, Park H, Park K. Polym Adv Technol 2000;11:617–25.
[22] Guilherme MR, Silva R, Girotto EM, Rubira AF, Muniz EC. Polymer 2003;44:4213–9.
[23] Ito K, Ujihira Y, Yamashita T, Horie K. Radiat Phys Chem 2000;58:521–4.
[24] Guilherme MR, da Silva R, Rubira AF, Geuskens G, Muniz EC. React Funct Polym 2004;61:233–43.
[25] Sannino A, Netti PA, Mensitiri G, Nicolais L. Compos Sci Technol 2003;63:2411–6.
[26] Sahiner N, Malci S, Celikbicak Ö, Kantoğlu Ö, Salih B. Radiat Phys Chem 2005;74:76–85.
[27] McGrath JL, Hartwig JH, Kuo SC. Biophys J 2000;79:3258–66.
[28] Muniz EC, Geuskens G. J Membr Sci 2000;172:287–93.
[29] Hickey AS, Peppas NA. J Membr Sci 1995;107:229–37.
[30] Hickey AS, Peppas NA. Polymer 1997;39:5931–6.
[31] Kuckling D, Harmon ME, Frank CW. Macromolecules 2002;35:6377–83.
[32] Stile RA, Healy KE. Biomacromolecules 2002;3:591–600.
[33] Liang L, Rieke PC, Liu J, Fruxell GE, Young JS, Engelhard MH, et al. Langmuir 2000;16:8016–23.
[34] Serpe MJ, Jones CD, Lyon LA. Langmuir 2003;19:8759–64.
[35] Dadhaniya PV, Patel MP, Patel RG. Polym Bull 2006;57:21–31.
[36] Zanjanchi MA, Sohrabnejad S. J Inclusion Phenom Macrocyclic Chem 2003;46:43–9.
[37] Zhang X-Z, Chu C-C. J Mater Sci 2003;13:2457–64.